Open Access Journal

Journal of Power Technologies 97 (5) (2017) 416–428

journal homepage:papers.itc.pw.edu.pl

Modeling of Warm-Keeping Process with Hot Air in Steam Turbines

Piotr Łuczyński[a,*], Dennis Többen[a], Manfred Wirsum[a], Wolfgang F. D. Mohr[b], Klaus Helbig[c]

[a] *Institute for Power Plant Technology, Steam and Gas Turbines, RWTH Aachen University, Templergraben 55, 52062 Aachen, Germany;*
[b] *General Electric (Switzerland) GmbH, Brown Boveri Str. 7, 5401 Baden, Switzerland;*
[c] *GE Power AG, Boveristraße 22, 68309 Mannheim, Germany*

Abstract

Steam turbines in conventional power plants have to deal with an increasing number of start-ups due to the high share of fluctuating power input in renewable power generation. As a result, the development of new methods for flexibility improvements—such as reductions in start-up time and the effects these start-ups have on turbine lifetime—have become increasingly important. In pursuit of this objective, General Electric has developed a concept for both the pre-warming and warm-keeping of a high-pressure (HP) / intermediate-pressure (IP) steam turbine with hot air: hot air is passed through the turbine while the turbine is rotated by the turning engine. Due to the high impact of transient flow phenomena on heat transfer during turbine warm-keeping operations, the reliable modeling of the time-dependent temperature distribution within thick-walled components is required as a tool for the optimization of these operations. Due to the extremely high computational effort required for conventional transient Conjugate Heat Transfer (CHT) simulations, alternative fast calculation approaches must be developed. The applied methodology for modeling warm-keeping turbine operations with hot air is presented in this paper. Furthermore, the key modeling steps have been analyzed. A fast transient CHT simulation approach called the Equalized Timescales (ET) method was developed to investigate heat transfer in the fluid and blades. Moreover, the setup of ET simulations was optimized with regard to accuracy and computing time. As a result, several operating points characterizing the turbine warm-keeping operational range were calculated for a single stage model. A sensitivity analysis regarding the heat transfer between fluids and solids was conducted to identify the most relevant surfaces. The ET method was then expanded to a numerical 3-stage turbine model in order to determine a HTC characteristic map for heat transfer in warm-keeping operations. This enables fast calculation of heat transfer rates and, consequently, computationally efficient determination of temperature distribution in warm-kept steam turbines. For comparison, the distribution of HTC was additionally calculated for one operating point of a 5-stage turbine model. Finally, the contact heat transfer in blade roots, which is believed to have a high impact on the temperature distribution of the rotor, was experimentally assessed in a test rig. The description of the test rig and the methodology of determination of the thermal contact resistance (TCR), as well as the impact of TCR on the temperature distribution in the rotor are presented.

Keywords: District heating networks; heat cost; optimum pipe diameter; graph theory

1. Introduction

In the past few decades the European energy market has been evolving dynamically. Out of concerns relating to the environment and climate change, the share of renewable energy sources (RES) in electricity generation has been constantly increasing. For almost all renewable resources, a key issue is variability and unpredictability; a sudden change in weather conditions can result in a power shortage and disturb the precarious balance in the energy system.

*Corresponding author
Email address: luczynski@ikdg.rwth-aachen.de (Piotr Łuczyński)

In addition, subsidized renewable electricity generation impacts the annual capacity of conventional power plants, originally designed for continuous work at base load. Hard coal fired power plants in particular already have to shut down on weekends for periods of up to 60 hours [1]. Consequently, a cold start-up is required afterwards.

The new operational pattern of conventional power plants negatively affects the lifetime of the turbine and leads to high thermal stresses in thick-walled components. Due to the high temperature difference between rotor and inlet steam temperature after a long period of inactivity, the stresses occurring in the HP and IP steam turbines are particularly critical. The typical start-up time of a turbine from cold state is estimated to be about five to eight hours [2]. Shortening this

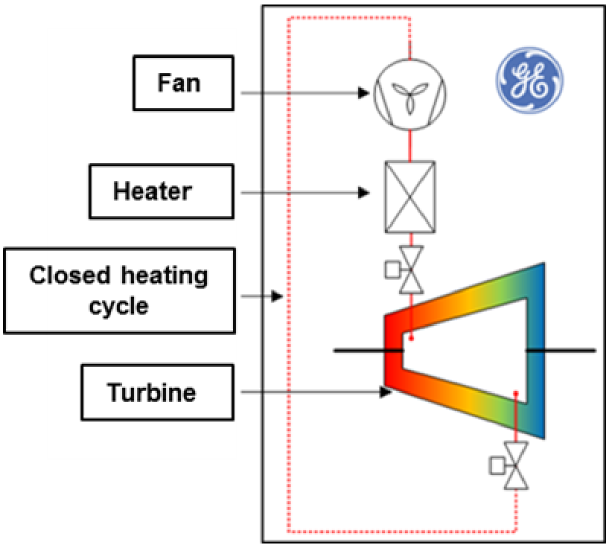

Figure 1: Warming arrangement for a steam turbine

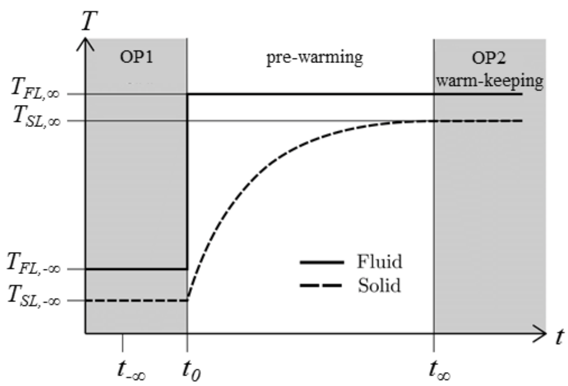

Figure 2: Behavior of fluid and solid temperatures in both pre-warming and warm-keeping operations

time and achieving steeper startup gradients with no negative effect on the lifetime of the turbine requires innovative technical solutions.

A conceivable method to reduce start-up time is the concept of turbine warm-keeping or pre-warming (depending on the technical execution). Warm-keeping solutions seek to minimize or compensate for heat losses that occur during periods of turbine inactivity. Apart from additional thermal insulation, the technical implementation of warm-keeping or pre-warming may be achieved by means of two basic solutions: application of heating blankets, or heating of rotor and casing with a hot working fluid. According to the investigation presented in [3], the concept of custom-tailored electric blankets implemented on a GE A10 steam turbine enabled a reduction in warm startup times of nearly 50%. Nevertheless, it should be mentioned that for a two-casing turbine, the effectiveness of rotor pre-warming is limited by air heat transfer resistance. An additional problem with the heat blankets method is the pre-warming of internal turbine components, like valves. In [4], the influence of heat blankets and higher

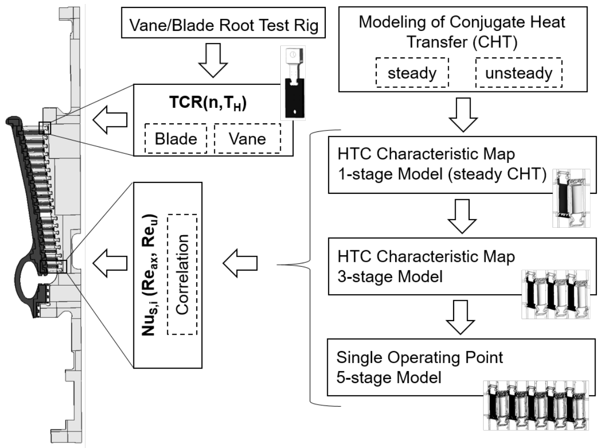

Figure 3: Modeling of warm-keeping process with hot air

gland steam temperature on turbine temperature in a solar power plant was analyzed. This research was subsequently extended in [5] on further methods for heating up the turbine with steam: gland steam pressure increase, back pressure increase and barring speed increase.

Finally, an innovative approach to heating or warm-keeping of the HP / IP steam turbine with hot air was presented in [6]. Warm or hot start-up conditions can be ensured even after long idle time by means of additional hot air warming cycles. This air is heated up by an electrical heater and passed through the turbine with the use of a fan while the rotor is continuously rotating, as presented in Fig. 1.

The two main advantages of this solution over the heat blankets method are: (i) an enhanced rate of heat transfer in the rotor that is independent of the number of turbine casings, and (ii) the possibility of effective pre-warming of additional armatures, like valves. The presented approach serves as a basis for the current investigations.

The main objective of this paper is to provide comprehensive knowledge about the methodology of modeling turbine warm-keeping processes that use hot air. Furthermore, the vital steps of the analysis, as well as the most important results of the conducted research, are discussed.

Due to the previously discussed purposes of the warm-keeping application, the heat transfer processes and the temperature distribution within the thick-walled turbine components in investigated off-design operations are of particular importance. The exponential growth of computing power in combination with advanced software tools enables the numerical investigation of heat transfer processes based on the Conjugate Heat Transfer (CHT) methods. The coupled solution of the energy equation in fluid as well as in solid domains is characterized by high accuracy and low user effort. Owing to the high computational cost, the CHT simulations are mainly used for steady state calculations. However, a time accurate calculation on the basis of the coupled method requires extreme computing resources, since the timescales of the convective and the conductive heat transfer differ by a factor of about 10 000 [7]. In view of the high turbulent flow nature that is observed in warm-keeping operations and flow structures typical for windage operation [8], an investigation of heat transfer in turbines requires unsteady calculation approaches, especially in multistage simulations. Therefore, based on the numerical model of the single turbine stage, an innovative approach called the Equalized Timescales (ET) method was investigated for warm-keeping modeling purposes. The ET calculation approach is known from research conducted in the field of thermal shock tests of turbochargers, presented in [9] and [10].

In contrast to the thermal shock approach, which theoretically could be applied for modeling of the pre-warming procedure, the temperature gradients occurring in warm-keeping operation are significantly smaller. Hence, due to the setup variation of ET simulations presented in this work, additional savings in computing time may be achieved. The principle difference in behavior of the fluid and solid temperatures in simply-modeled pre-warming and warm-keeping operation is shown in Fig. 2.

Using the ET method, the single stage model, in addition to the 3- and 5-stage models, could be investigated by means of unsteady CHT simulations. For a detailed analysis of a broad operating range, and to summarize the heat transfer processes in the turbine channel, the various CHT-Simulations of a single IP steam turbine stage are performed to provide a characteristic HTC-map for warm-keeping operations. Simulations of multistage models should deliver information about the differences in HTC distributions between particular turbine stages. The long-term project objective is to develop a correlation describing HTC-courses as a function of dimensionless numbers such as the Reynolds-number. Moreover, the determined HTC may be used for further improvements in start-up procedures.

In order to reliably calculate the temperature distribution in a warm-kept steam turbine, the thermal contact resistance (TCR) on the relevant surfaces must also be considered. According to the study presented in the following sections, over 90% of all exchanged heat in warm-keeping operation is transferred from hot air to blade and vane. As a result, the impact of thermal contact resistance (TCR) on rotor and housing temperature values increases remarkably. Therefore, in pursuit of TCR determination, a specially designed test rig was developed. The measured thermodynamic parameters enable analytical and numerical calculation of the values of TCR for particular contact surfaces. In order to assess the influence of TCR on rotor temperature, additional FEM calculations with TCR values determined for different rotational speeds were conducted and evaluated. The graphical representation of the described investigation steps is shown in Fig. 3.

The numerical models used for warm-keeping investigations are presented in Section 2. The ET calculation approach as well as the investigation of ET setup variation is given in Section 3. This is followed by the analysis of heat transfer in single and multistage turbine models in Section 4. The description of the test rig and TCR determination as well as the evaluation of TCR impact on the rotor temperature are provided in Section 5. Section 6 contains the conclusion.

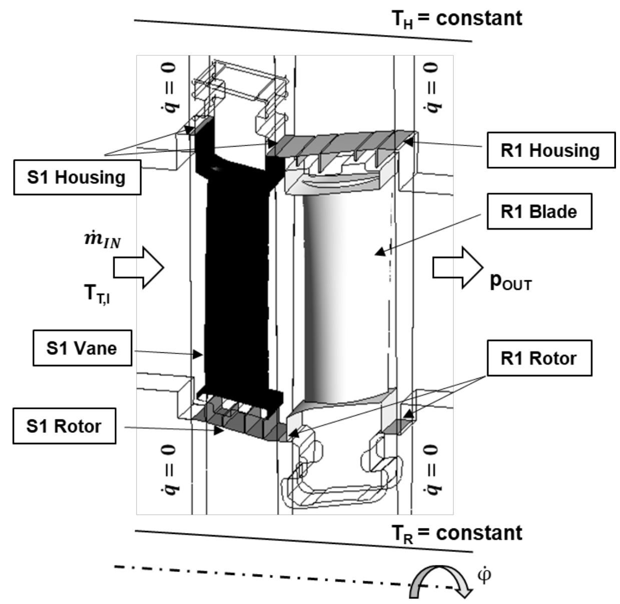

Figure 4: Numerical single stage model with surface denotation

2. Numerical model

In cooperation with the industrial partner General Electric, a numerical model of a single repetitive turbine stage has been developed in order to calculate several discrete operating points (OPs) and to determine values of HTC covering a wide range of investigated warm-keeping operations. Due to the high steam temperature, thermally induced stresses arise particularly within the first turbine stage. The heat transfer investigation focuses on a single stage model. As depicted in Fig. 4, one blade passage (approx. 2.5°) of the turbine wheel is modeled by means of circumferential periodic boundary conditions. In the case of steady state simulations, the transformation from the non-rotating to the rotating system is performed by Frozen Rotor Interface in order to capture the strong backflows through the domains interface. The constant temperature of the surface of the predefined concentric hole in the rotor, and of the outer surface of the inner steam turbine casing, are represented by T_R and T_H respectively. The temperature values are approximately 45% of the live steam temperature at nominal load. The axial walls of the model are considered to be adiabatic. For boundary conditions of fluid state, the mass flow and total temperature at inlet are varied depending on the OP. In outlet planes a constant static pressure is applied. The hexahedral mesh of all single stage turbines consists of approximately 6.8 million nodes. 3.6 million nodes are located in the fluid state and 3.1 million nodes discretize the solid body. In the fluid boundary layer, the dimensionless wall distance y^+ is lower than 1. A mesh study was conducted to ensure that the results are unaffected by the mesh quality. To model the turbulence in the thermal sub layer, the low Reynolds $k\omega$-SST turbulence model is used. Furthermore, the fluid state is assumed to be a fully turbulent ideal gas with constant fluid properties. Constant material properties are also applied for the solid state. A more detailed description of the investigated single stage model as well as its verification and comparison to data presented in the literature can be found in [8]. In the case of multistage simulations, the single axial repeating stage is extended to a 3- and 5-stage turbine model by duplication.

Based on similarity theory, the heat transfer conditions in warm-keeping operation, as well as the flow in the turbine, may be characterized by means of dimensionless numbers. For the purpose of the evaluation of heat transfer through each interface between solid and fluid state (Fig. 4), an average heat transfer coefficient $\alpha_{i,n}$ is defined in Eq. 1:

$$\alpha_{i,n} = \frac{\dot{Q}_i}{A_i(\overline{\overline{T}}_n = \overline{T_i})} \tag{1}$$

The index i refers to the individual surface and the index n to the inlet plane of the flow channel section in which the regarded blade/vane row is located. $\dot{Q}_i$ is the area averaged heat rate of the surface i with the surface area A_i. The reference temperature $\overline{\overline{T}}_n$ is the mass flow averaged temperature of the fluid passing through the plane n. $\overline{T}_i$ is defined as the area averaged temperature of the surface i. Furthermore, the Nusselt-Number can be expressed as a function of HTC, the characteristic length for heat transfer $\overline{s}$, calculated on basis of chord length, and the thermal conductivity (determined at the mean flow temperature):

$$Nu_{i,n} = \frac{\alpha_{i,n} \cdot \overline{s}}{\lambda_{air}} \tag{2}$$

Considering the input parameters 'air mass flow rate' $\dot{m}$ and 'rotational speed' φ, the fluid flow may be characterized by additional dimensionless numbers like the Reynolds number in axial flow direction (Eq. 3) and in circumferential direction (Eq. 4). The radii r_1 and r_2 describe the position of the inner and outer wall of the flow channel. In order to define the Reynolds number, the characteristic length l_i of the regarded surface and the kinematic viscosity (calculated at the mean flow temperature) are used. As reported in [8], for thermodynamic and economic reasons, the warm-keeping turbine operations are realized by low hot air volume flows. Therefore, depending on the rotational speed and mass flow rate, the fluid field is changing. The investigated fluid flow can be characterized by the following relationships:

$$Re_{ax} = \frac{\dot{m} \cdot l_i}{\rho\pi(r_2^2 - r_1^2) \cdot \nu_{air}} \tag{3}$$

$$Re_u = \frac{\pi \cdot \varphi \cdot (r_1 \dot{+} r_2) \cdot l_i}{60 \cdot \nu_{air}} \tag{4}$$

$$\Phi = \frac{c_m}{u} \cong \frac{c_{ax}}{u} = \frac{Re_{ax}}{Re_u} \tag{5}$$

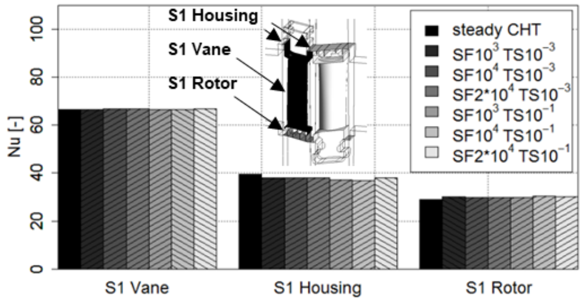

Figure 5: Nusselt-number at S1 surfaces for different values of SF and TS

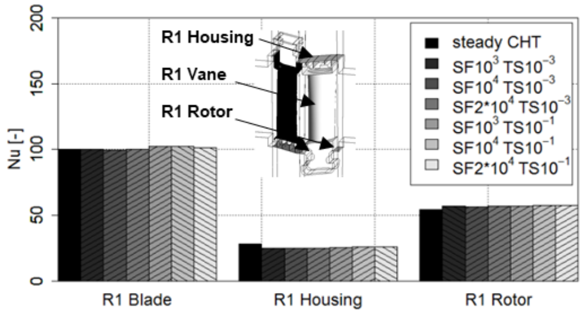

Figure 6: Nusselt-number at R1 surfaces for different values of SF and TS

3. Modeling of conjugate heat transfer

The primary objective of numerical heat transfer simulations in the field of turbo machinery is to accurately determine solid body temperatures. Although much effort has already gone into developing conjugate heat transfer (CHT) methods, coupled solutions of fluid convection and solid conduction are mainly confined to steady simulations. These result in typical numerical dilemmas concerning additional assumptions with regard to neglecting flow nonlinearities and achieving satisfying convergence. Particularly in turbine flows found in extremely off-designed OPs such as warm-keeping operations, the unsteady simulation approach is vi-

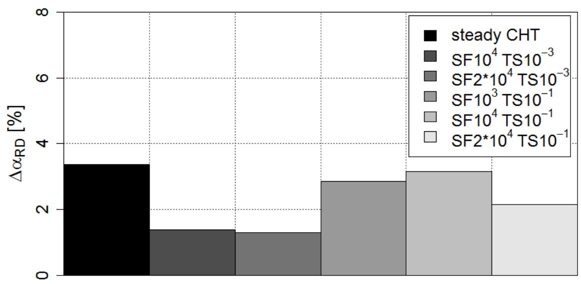

Figure 7: Averaged relative deviation of HTC for different values of SF and TS (ref. calculation SF1000 TS 0.001 s)

tal for quality results.

The two main calculation approaches of transient fluid/solid heat transfer modeling described in academic publishing can be divided into two families. In the conventional CHT method, a CFD calculation is iteratively coupled with a conductive FEA calculation. Owing to the solution of the energy equation at the fluid/solid interface, the continuity of the temperatures and heat rates at coupled boundaries is ensured. Examples of this method can be found in [11] and [12]. Another innovative possibility of CHT modeling based on the Fourier transform at the fluid/solid interfaces is presented in [7].

The second approach relies on the assumption of a linear relationship between the convective heat rates across the boundary layer and the driving temperature differences. In other words, the heat transfer coefficients are assumed to be constant. In this method the HTCs are obtained in CFD simulations and subsequently used as boundary conditions for FEA calculations. A major difficulty of the uncoupled approach is a proper definition of fluid temperatures, which in the optimal case should be associated with the fluid thermal boundary layer. The global definition of the reference fluid temperature inhibits the capturing of secondary flow phenomena relevant to the local heat transfer. Examples of this method are the heat transfer calculations of the rotor stator cavities published in [13] and [14]. The uncoupled approach is considered to be the computationally time efficient method, since no iterative solution is required at the fluid/solid boundary. Unfortunately, research shows that uncoupled methods lead to high inaccuracies, especially when calculating heat transfer in housing cavities. Due to the high temperature of rotating blades, the direction in which heat is transferred through blade shroud surfaces partially reverses. As a result, the assumption of constant HTCs negatively influences calculation stability and the quality of results. Therefore, in order to accurately calculate high turbulent flow in warm-keeping operations, a coupled method is required.

As previously mentioned, a time accurate CHT simulation is characterized by extreme computational effort, since the timescales of the conductive and the convective heat transfer differ by a factor of 10 000 [7]. Considering the numerical stability analysis, the following inequalities can be formulated for a simplified 1D fluid/solid system [7]:

$$Fluid\,domain\,(CFL-number) \qquad \frac{\Delta t_f V}{\Delta x} < 1 \tag{6}$$

$$Solid\,domain\,(Fourier-number) \qquad \frac{\Delta t_s a}{\Delta x^2} < 1 \tag{7}$$

The solution of both relations (Eq. 6, Eq. 7) for the typical values of fluid/solid properties and mesh spacing Δx presented in [7] leads to:

$$\frac{\Delta t_{SL}}{\Delta t_{FL}} \approx 10000 \tag{8}$$

Thus, the ratio of the timescales of the conduction and the convection process from the perspective of numerical stability may also be estimated on a factor of about 10^4. A fully coupled transient heat transfer calculation would hence lead to very high calculation times, because a long conduction process would have to be calculated with very small time steps of approximately 10^{-3} to 10^{-5} s. Under these circumstances, a numerical simulation of a 10 minute heating up process of a small radial turbine would lead to calculation times of more than 100 years, as reported in [15]. Additional simplifications must therefore be made. In the following considerations, the Equalized Timescales method (ET) known from numerical simulations of thermal shock in turbochargers (presented in [9] and [10]) is investigated for modeling warm-keeping turbine operations. In order to explain the main principles of the ET approach, a simple analytical method is evaluated. Essentially, for a heated solid body with a homogenous temperature distribution, the following equation describing time-dependent temperature changes can be formulated:

$$\rho_{SL} c_{p,SL} V_{SL} \frac{\partial T_{SL}}{\partial t} = -A_{SL}\alpha(T_{SL} - T_{FL}) \tag{9}$$

Assuming constant material properties, HTC and fluid temperature over time, the integration of Eq. 9 leads to the following relationship:

$$\begin{aligned} T_{SL} &= (T_{SL,0} - T_{FL})e^{-\frac{\alpha A_{SL}}{c_{p,SL}\rho_{SL}V_{SL}}t} + T_{FL} \\ &= (T_{SL,0} - T_{FL})e^{-\tau \cdot t} + T_{FL} \end{aligned} \tag{10}$$

$$with\,\tau = \frac{\alpha A_{SL}}{c_{p,SL}\rho_{SL}V_{SL}} \tag{11}$$

The value of the exponent τ expresses the time scale of the heating process. The main idea behind the ET method is to equalize the time scales of the fluid and solid by reducing the specific heat $c_{p,SL}$ of the solid body by the speed up factor SF. Furthermore, for the simplified case, the modified time of heating process t^* can be associated with real time by means of Eq. 13.

$$c^*_{p,SL} = \frac{c_{p,SL}}{SF} \tag{12}$$

$$t^* = \frac{t}{SF} \tag{13}$$

The ET method allows for significant acceleration in the numerical calculation of unsteady CHT processes. In order to assess the suitability of the described approach for the determination of the transient thermal behavior of the fluid/solid system, the Fourier and Biot numbers are used. As reported in [16], transient temperature fields of the same geometry and the same boundary conditions are similar if the Biot Number and Fourier Number are equal:

$$\begin{aligned} Fo &= \frac{\lambda_{SL}t}{c_{p,SL}\rho_{SL}l^2} = \frac{\lambda_{SL}t^* SF}{c^*_{p,SL}SF\rho_{SL}l^2} \\ &= \frac{\lambda_{SL}t^*}{c^*_{p,SL}\rho_{SL}l^2} = Fo^* \end{aligned} \tag{14}$$

$$Bi = \frac{\alpha l}{\lambda_{SL}} = Bi^* \tag{15}$$

Assuming constant HTC, in addition to the implementation of modified specific heat $c^*_{p,SL}$ and time t^* into the definition of both dimensionless quantities, the said quantities do not change their values for a simplified case. As presented in [9] and [10] the greatest impact of the chosen speed up factor and time step is observed during the first phase of the thermal shock process. Furthermore, the following rule can be applied in the characterization of the ET approach: the smaller the value of SF and time step (TS), the more accurate the solution of transient temperature fields can be expected. For the modeling of turbochargers, the values of SF equal to 1000 proved themselves a reliable choice for the setup of unsteady calculation [10].

In the case of warm-keeping operations, due to the smaller temperature gradients between fluid/solid states, the higher values of SF may lead to accurate solutions. As a result of the significant computational time saving, this would allow several unsteady multistage calculations to be carried out and hence, expand the range of investigated OPs.

In order to verify the ET method and to investigate the setup of unsteady simulation, additional research was conducted. Using a single stage turbine model, the steady CHT calculation of one OP was compared with the results of unsteady simulations, each run with different values of speed up factor and time step. The Nu-numbers defined for each fluid/solid interface (cp. Fig. 4) are presented for stator and rotor domains in Fig. 5 and Fig. 6 respectively. By comparison, the relative deviation of HTC values is determined by means of Eq. 16:

$$\Delta\alpha_{RD} = \sum_i \left| \frac{\alpha_i - \alpha_{SF1000,i}}{\alpha_{SF1000,i}} \right| \frac{A_i}{A_{tot}} \tag{16}$$

As expected, only a slight difference in calculated values of Nu-numbers for all unsteady simulations can be observed. Considering the simulation with SF 1000 and TS 0.001 s as a reference calculation, the highest deviation in HTC values (Fig. 7) and hence in Nu-numbers occurs in the steady state CHT method—over 3%. This may be explained by obvious differences between RANS/URANS calculation approaches, unequal types of rotor-stator interfaces and better convergence of unsteady simulations. Furthermore, the increasing value of TS negatively influences the quality of the results and considerably decreases the number of investigated rotor-stator positions as the blade passes through the flow channel. Therefore, an unsteady ET simulation with SF 20 000 and TS 0.001 s as a setup parameter appears to be a good compromise between computing effort and accuracy of the calculation. Due to the great amount of numerically depicted OPs, the single stage turbine model is calculated by means of steady simulations. With regard to the mentioned inevitability of an unsteady CHT approach for multistage investigations, the ET method with SF 20 000 and TS 0.001 s is used to calculate 3- and 5-stage OPs. In the following section, the mass flow and rotational speed of each OP are expressed by Re-numbers $Re_{ax,in}$ and $Re_{u,in}$ determined with Eq. 3 and Eq. 4 for the flow parameters at the inlet of the turbine.

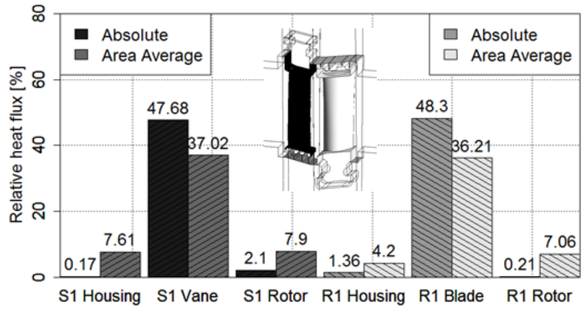

Figure 8: Relative heat rate for main surfaces

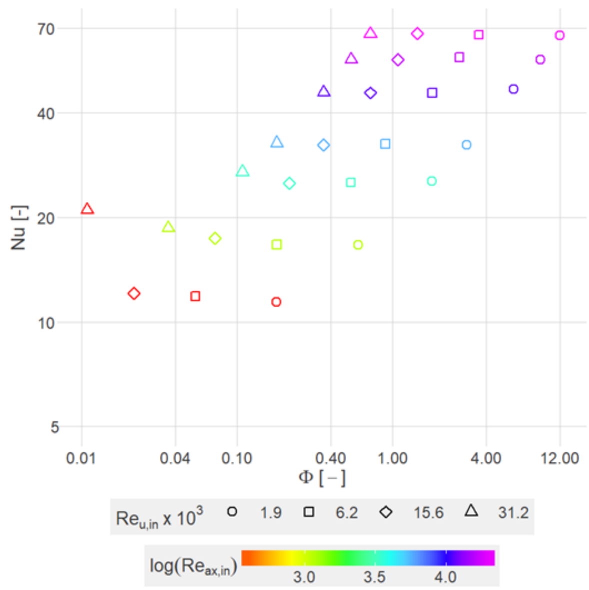

Figure 9: Nusselt-number at S1 Vane surface of the single-stage model

4. Heat transfer in warm-keeping operations

According to heat transfer principles, the thermal energy transfer processes may be classified into three basic mechanisms: conduction, convection and radiation. In warm-keeping operations, the convective heat rate has a major impact on heat transfer between working fluid and turbine components. Due to the thermal boundary conditions of CHT models, the temperatures of all solid surfaces in the flow channel are similar in comparison to the temperature difference between fluid and solid. Therefore, the influence of heat radiation can be neglected with good approximation. Furthermore, the effect of conduction within air is also considered to be negligible. Thus, in order to evaluate the convective heat transfer, the percentage of the total heat rate exchanged through each fluid/solid interface (cp. Fig. 4) is

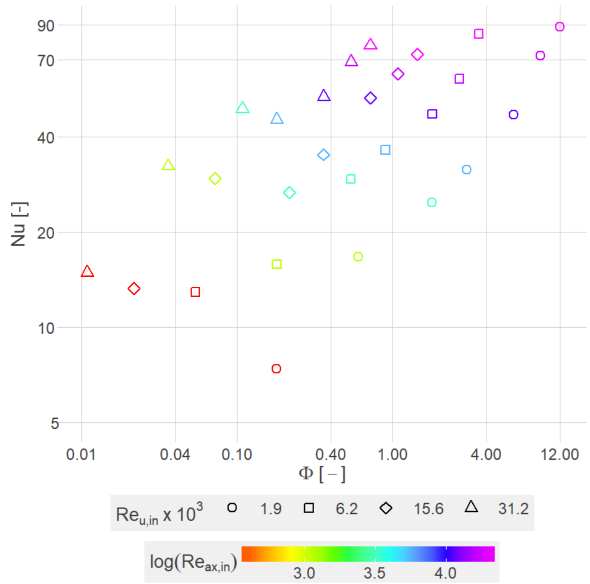

Figure 10: Nusselt-number at R1 Blade surface of the single-stage model

presented in Fig. 8. Contrary to conventional turbine operations, slower leakage flow velocities—over 90% of total heat rate averaged over all simulations—are exchanged through vane and blade surfaces, due to less leakage flow through the cavities.

The investigation presented in this work therefore focuses on the Nu-numbers calculated for vane and blade fluid/solid interfaces. The values of Nu-numbers obtained for S1 Rotor and R1 Housing surfaces can be found in [8]. The heat transferred through S1 Housing and R1 Rotor is negligible.

The Nu-numbers determined for S1 Vane and R1 Blade surfaces are given in Fig. 9 and Fig. 10. For the purpose of evaluation, the Nu-numbers obtained for each OP are marked with colored symbols, indicating the values of Re-numbers $Re_{ax,in}$ and $Re_{u,in}$, as well as their ratio—flow coefficient φ. Due to the non-rotational inflow at the first vane row, the influence of the rotational speeds on vane Nu-numbers is generally low. The rotational impact gains in importance only for smaller values of $Re_{ax,in}$. Similar trends may also be observed for blades. In particular, the small mass flow rates on the edge of windage turbine operations lead to enhanced heat transfer for higher $Re_{u,in}$ values. In conclusion, the values of the Nu-numbers for the increasing flow coefficients may be defined as the function of Re-numbers $Re_{ax,in}$, solely in the axial direction.

In Fig. 11 the results of the unsteady multistage investigation are provided. The notation RN refers to the same surface, with the value of N indicating the stage in which the surface is located. For example, surface R2 is the surface R1 depicted in Fig. 4, but in the second stage. Both diagrams located in the left column of Fig. 11 depict the Nu-numbers of the 1-stage and 3-stage models, presented for the S1-S3/R1-R3 vane/blade surfaces and calculated for a constant $Re_{u,in}$. Additionally, a single OP of the 5-stage model is included. Interestingly, the values of Nu-numbers [Nu($Re_{ax,in}$, $Re_{u,in}$ = const.)] at the S1 vane obtained in 1- and 3-stage simulations are almost identical. The similar Nu-numbers on the S2 and S3 vane surfaces differ from the S1 values due to the low turbulence of inflow at the first vane row. In contrast, the differences between values of Nu-numbers determined at each R1-R3 blade surfaces are smaller. Generally, the sudden kinks in the Nu-curves of the 1- and 3-stage models may be explained by the impact of secondary flow phenomena on the local heat transfer (cp. [8]).

Furthermore, the detailed investigation of a single OP is given in the middle and right column of Fig. 11. The results of the 5-stage model confirm the slightly different heat transfer conditions on the first vane row, as well as the similar values of Nu-numbers on the S2-S5 and R1-R5 surfaces. Moreover, the Nu-numbers calculated in the 5-stage model are on average about 5% and 6% higher for S and R surfaces respectively, compared to those obtained in 1-stage simulations. Thus, the 1-stage model calculates the heat transfer with good approximation and may be used to develop the HTC correlation as a function of Re-number.

5. Blade root test rig

The study of heat transfer presented in the previous section, and graphically depicted in Fig. 8, reveals that in warm-keeping operations most of the thermal energy transferred from hot air to thick walled casing/rotor has to overcome the thermal contact resistance at vane/blade roots. Therefore, knowledge of the TCR values for different turbine OPs is essential for proper modeling of temperature distribution in rotor and casing. There are several experimental and analytical approaches known in literature that can determine the values of the TCR. One of the first pieces of research concerning this topic was conducted as part of investigations into heat transfer performed for the space industry and presented in [19, 20, 21]. Further analytical approaches based on the investigation of flat surfaces characterized by different levels of roughness can be found in [22]. An extensive analysis and summary of TCR research conducted during the last few decades is provided in [18] and [23]. The results were detailed in work described in [24, 25]. The determined experimental values, in addition to the developed analytical model based on the calculation of real contact area, allows one to describe the TCR as a function of roughness, material structure and the contact pressure. Moreover, the obtained results provide an explanation concerning occasional large deviations in TCR values reported by different authors in the literature.

The results of TCR investigation presented in this paper are based on the experimental and numerical research described in [17]. In the first step, due to the rotational speed dependency of TCR and specific importance of rotor temperature in warm-keeping operations, hammer-head blade root geometry is used. As the main factors affecting the heat transfer contact pressure (which is associated with rotational

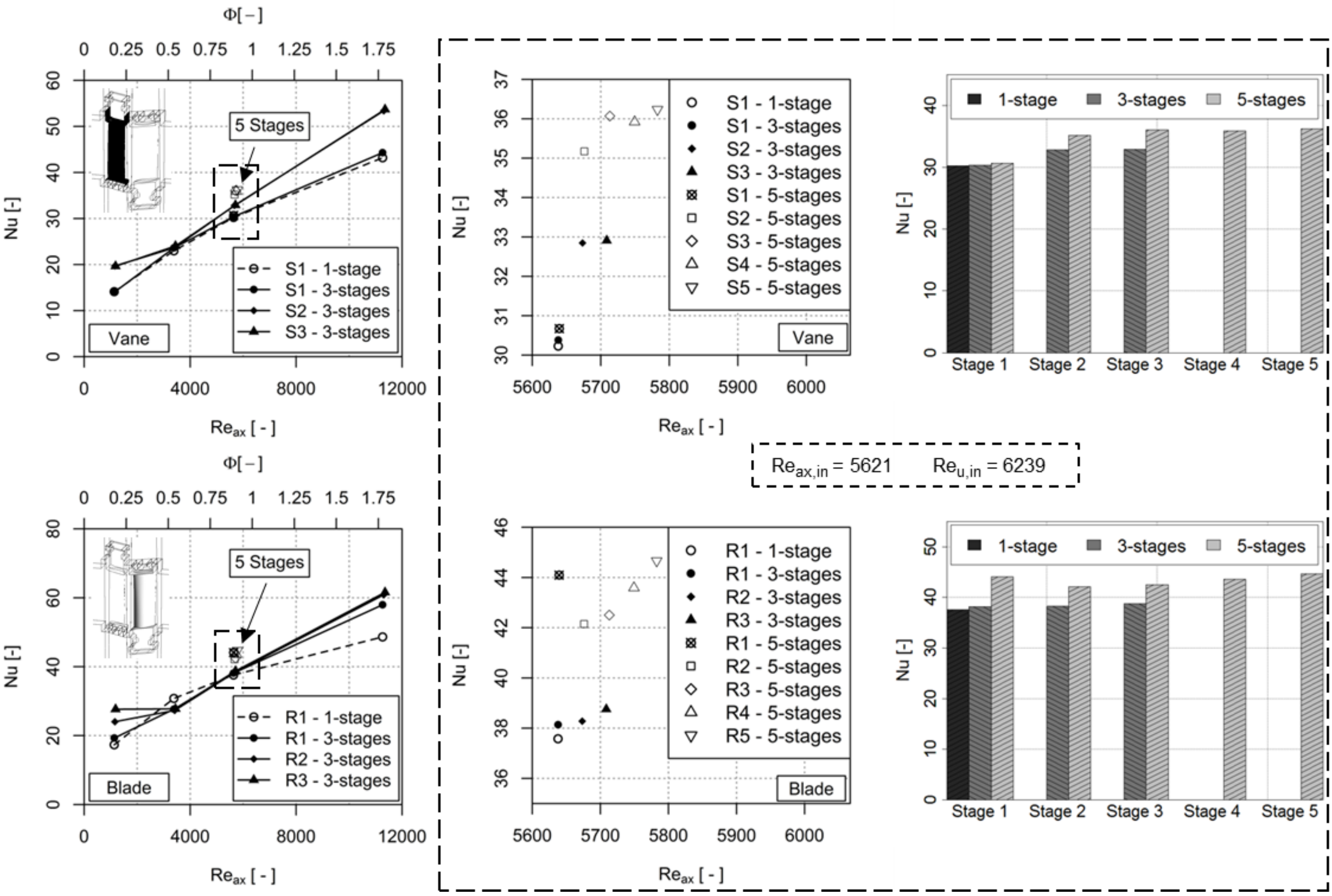

Figure 11: Nusselt number at vane (above) and blade (below) surfaces for constant rotational speed (left) and single OP (middle, right)

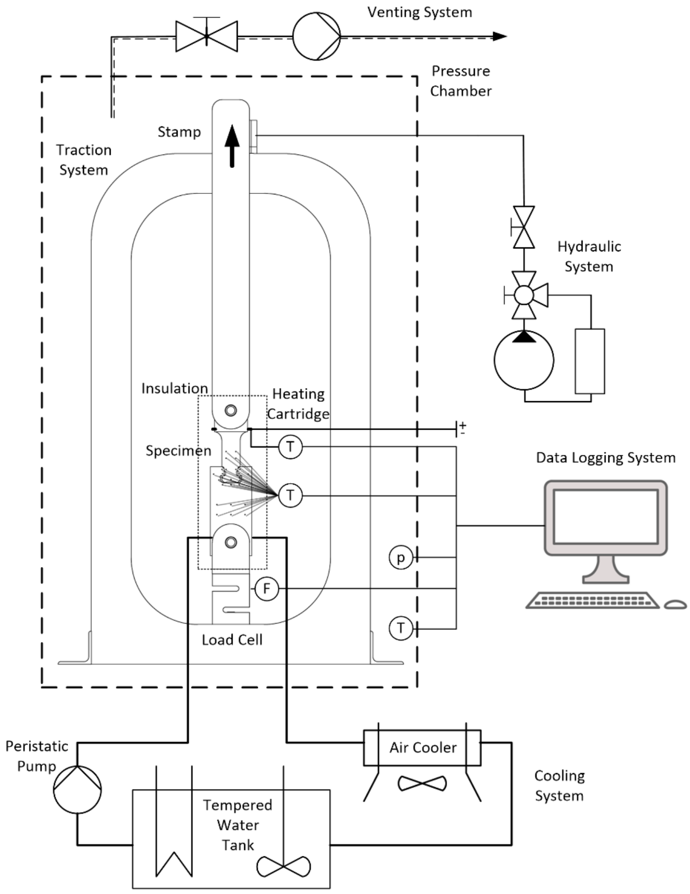

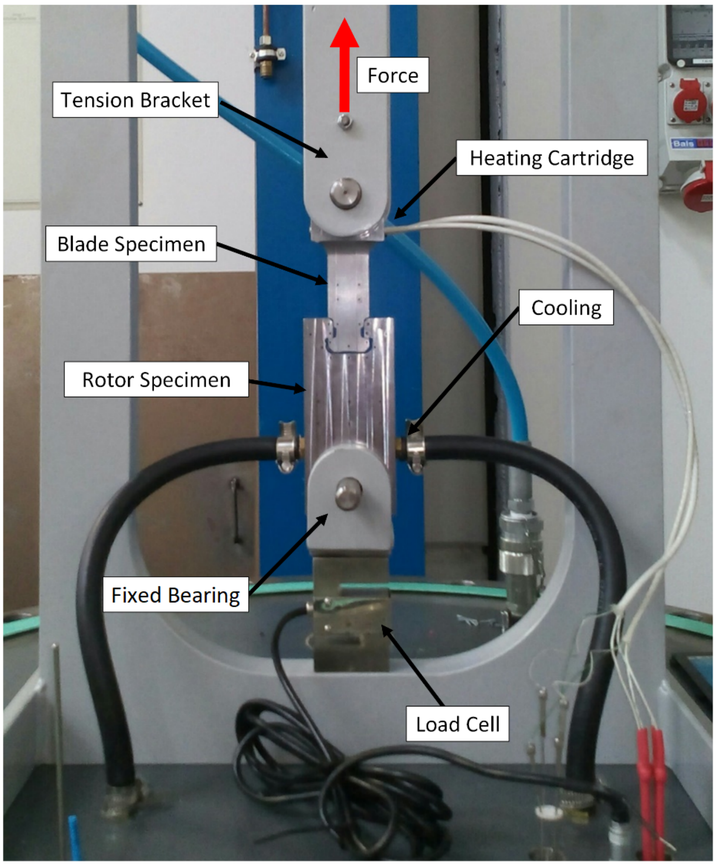

Figure 12: Schematic diagram of test rig (left) and installed specimens (right) [17]

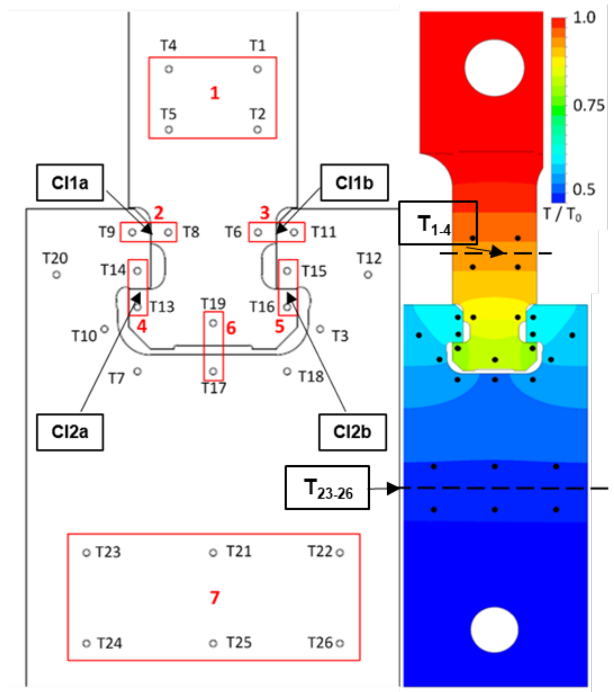

Figure 13: Metering positions with marked contact interfaces (CI) and temperature distribution in specimens

speed) have been considered, through subsequent numerical calculations, the impact of heat radiation in air pockets can also be evaluated.

A schematic diagram of the constructed test rig designed for experimental determination of TCR values, in addition to the installed specimens, is shown in Fig. 12. The centerpiece of the test rig is a traction system allowing the application of force of up to 10 kN to the blade specimen by means of a hydraulic pump, whilst the rotor specimen is held in fixed bearing. The traction system stands on the ground plate of a pressure chamber, which in combination with a vacuum pump allows variations in the ambient pressure as well as minimization of the heat losses to the environment. The operating conditions of the chamber cover a pressure range from 30 hPa to 3000 hPa. The heat flow in the blade and rotor specimen is generated using two heating cartridges (315 W each) and a cooling drill, as presented in Fig. 12. The cooling circuit consists of a temperature-controlled water tank, a high precision peristaltic pump and an air cooler. In this way, reproducible measurements can be ensured independent of the ambient conditions. The geometry of the blade and rotor test specimen was optimized for the tensile test and, hence, temperatures of over 250°C in contact surfaces as well as the necessary tensile force can be simultaneously investigated. The design of the blade root remains largely unchanged, though the individual surfaces were slightly modified. In test specimens, 26 Type-N thermocouples were installed in order to accurately capture the temperature distribution, as shown in Fig. 13.

The thermocouples group 1 (T1–T4) and 7 (T21–T26) were used to determine the incoming and outgoing thermal

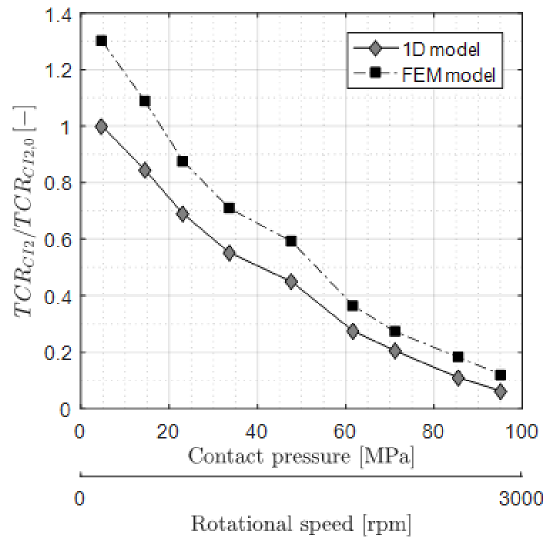

Figure 14: Values of TCRCl2 [18]

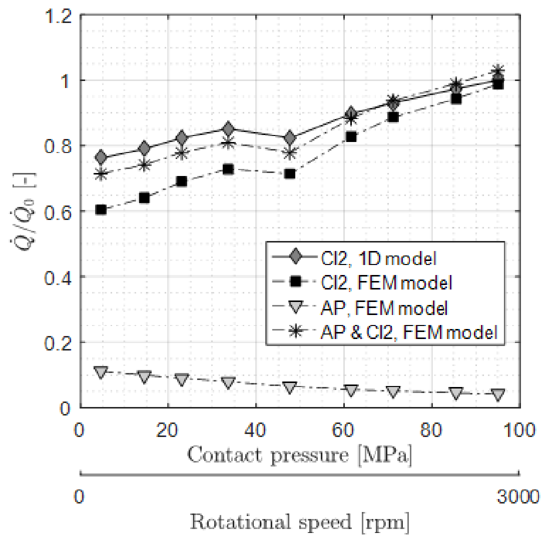

Figure 15: Heat rates in FEM and 1D model [17]

energy fluxes. Furthermore, the thermocouples group 2 to 6 served to calculate the heat transfer at the blade-rotor contact surfaces. The remaining measuring points were required for model validation. In addition to temperature values, various parameters describing the boundary conditions of the experiment were measured, such as the pressure and temperature of air in the chamber and the temperature of the heating cartridges and cooling water.

For the purpose of evaluation, a numerical FEM model in addition to a simplified one-dimensional (1D) approach were developed to calculate the TCR. An FEM model recorded the multidimensional heat transfer in solid states and air pockets. The 1D analytical approach serves as a comparison and verification for numerically obtained TCR values.

Direct measurement of the thermal contact resistance was not possible and it was therefore calculated based on the local temperature difference between contact surfaces ΔT_C

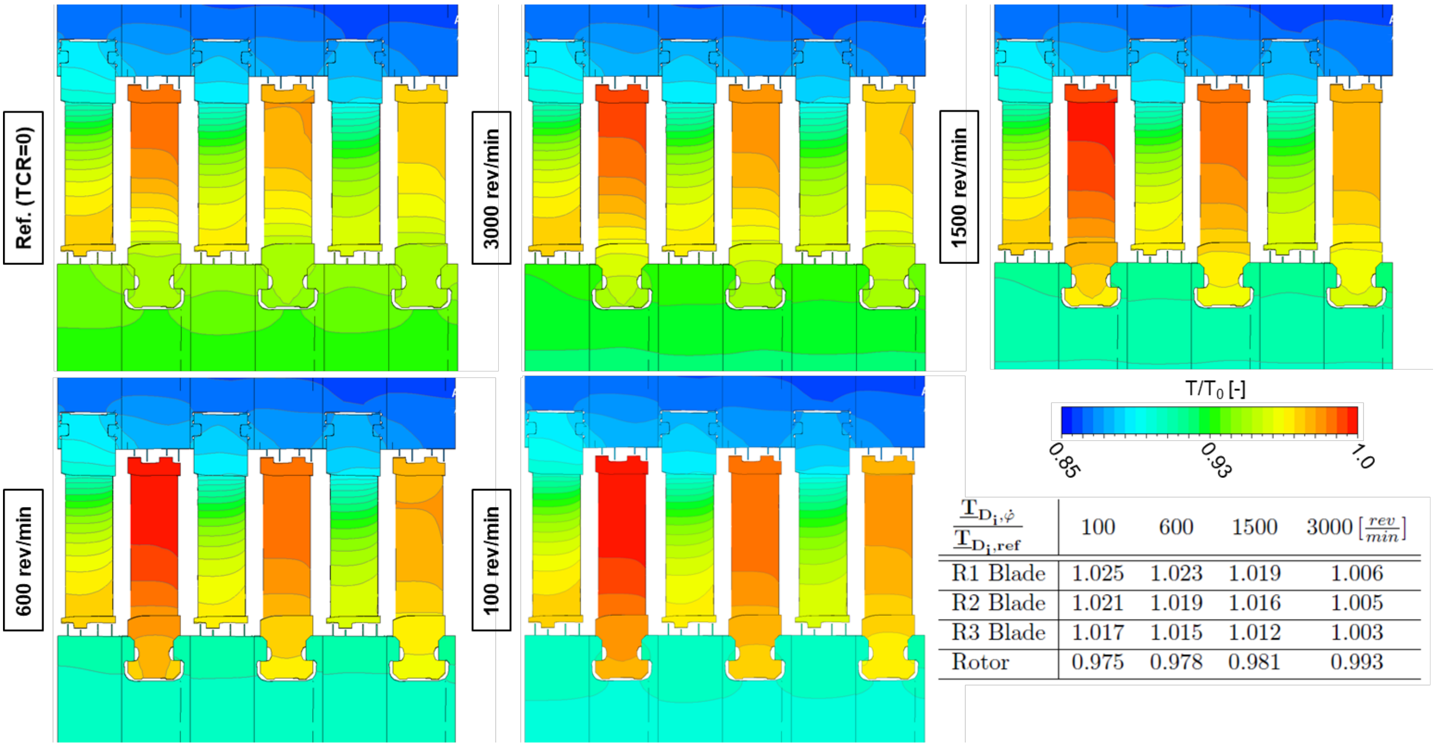

$\frac{T_{D_i,\dot{\varphi}}}{T_{D_i,ref}}$	100	600	1500	3000 $[\frac{rev}{min}]$
R1 Blade	1.025	1.023	1.019	1.006
R2 Blade	1.021	1.019	1.016	1.005
R3 Blade	1.017	1.015	1.012	1.003
Rotor	0.975	0.978	0.981	0.993

Figure 16: Impact of TCR on rotor temperatures in warm-keeping operations

and heat rate $\dot{Q}$ (Eq. 17):

$$TCR = \frac{A_C \cdot \Delta T_C}{\dot{Q}_C} \tag{17}$$

Considering the distance between measuring points in thermocouples group 2–5 (cp. Figure 13) and blade/rotor contact surfaces, the TCR values can be approximated analytically. To reduce the relative measurement error, the position of thermocouples ensures a sufficiently large temperature difference alongside a low distance to contact surfaces. Thus, a simple 1D analytical equation based on the material conductivity and Fourier's law delivers information about the temperature values on both sides of contact surfaces. In contrast to the 1D model, the FEM simulation allows one to iteratively determine the thermal contact resistance as well as to re-compute the temperature distribution in rotor and blade specimens. As an optimization criterion for iterative calculation loops, the minimum deviation between numerically obtained temperatures and measured values in positions T9, T11, T14 and T15 is chosen. The average measured temperatures T_{1-4} and T_{23-26} (cp. Fig. 13) serve as boundary conditions for FEM simulation. Furthermore, in all air pockets the radiative heat transfer is calculated by means of the Monte Carlo method. More details concerning experimental as well as numerical setup can be found in [17].

For the presented investigation, the specimen's geometry was modified in order to create an additional air pocket between axial contact surfaces CI1a and CI1b. Consequently, the impact of centrifugal forces on radial contacts CI2a and CI2b can be analyzed. The averaged CI2 values calculated for a single series of measurement with evacuated atmosphere and heating cartridges temperature equal to 150°C are given in Fig. 14. In the case of FEM simulations, all the calculated temperatures at measurement points are in good agreement with experimental data. The maximum deviation averaged for the measurement series was 2°C. As shown in Fig. 14, the TCR values determined by means of an FEM Model are higher than the contact resistance calculated by the 1D approach. To explain this difference, the heat rates through the air pockets (AP) and contact interfaces (CI) must be analyzed. According to the results presented in Fig. 15, the transferred radiative energy influences the amount of energy exchanged by conduction processes, and the radiation in AP is therefore responsible for the higher values of TCR obtained by the FEM approach. Moreover, the share of radiation energy decreases with higher contact pressure, which confirms the trend of TCR plots in Fig. 14. To conclude, the proposed FEM approach delivers time-efficient and accurate determination of TCR and temperature distribution in analyzed specimens.

Finally, in order to assess the impact of the TCR on the rotor temperatures, an additional FEM model based on the results and boundary conditions of previously analyzed CHT calculations was developed. The heat transfer on fluid/solid interfaces was modeled using constant HTCs known from the multistage CHT simulation. Furthermore, depending on the rotational speed, the value of TCR on radial contact surfaces was varied. As a reference, a simulation using FEM calculation with TCR equal to 0 was performed. The results of the investigation are graphically summarized in Fig. 16.

As presented, the temperature difference between blades and rotor decreases at higher values of rotational speeds. At the slowest rotational speed, the volume averaged rotor temperature was about 97.5% of the equivalent temperature value obtained in the reference calculation, neglecting thermal contact resistance. Furthermore, for all considered rotational speeds, the highest impact of TCR on blade temperatures is observed for the first turbine stage. This may be explained, as the highest heat transfer rates through the fluid/solid interfaces occur in the first blade row. The volume averaged temperatures for the R1 Blade domain achieve up to 102.5% of the reference temperatures.

The presented analysis reveals the high importance of the TCR for the investigation of turbine warm-keeping operations. Therefore, thermal contact resistance should be considered an important part of the analysis of warm-keeping processes.

6. Conclusion

In the presented work, a concept of turbine warm-keeping process using hot air was introduced. It included a detailed description of a modeling approach for investigations of heat transfer in warm-keeping operations. For the purpose of unsteady conjugate heat transfer simulations, a numerical approach called the Equalized Timescales (ET) method was analyzed to calculate the highly turbulent turbine flows and complex heat transfer phenomena. In the ET approach, the calculation time is reduced by modifying the specific heat of the solid state in order to equalize the timescales of fluids and solids. Consequently, the optimal values of speed-up factor (SF) and the numerical time steps (TS) regarding the accuracy and computing resources were identified, resulting in unsteady CHT simulations of multistage models. In the next step the rate of heat transfer on numerous fluid/solid interfaces for various values of Nu-numbers were analyzed. Due to the slow flow velocities in turbine cavities, more than 90% of the thermal energy in warm-keeping operations is transferred through blade and vane surfaces. Thus, the contact resistance in blade/vane roots is of particular importance. For a single stage model, 28 discrete warm-keeping OPs were calculated and subsequently compared with several multistage simulations. The results obtained by means of 3- and 5-stage unsteady calculations revealed a similar trend to the single stage simulations in the values of Nu-numbers Nu(Re_{ax}, Re_u) on blade and vane surfaces. Due to the different inflow conditions, the heat transfer process on the first vane row differs slightly from the heat transfer in the other repetitive turbine stages. From the second turbine stage, the heat transfer conditions repeat cyclically for the particular fluid/solid interfaces.

1D analytical approach and numerical FEM models have been presented, tasked with determining thermal contact resistance in the developed test rig. The values of TCR were evaluated as a function of contact pressure, which is directly associated with rotational speed. The obtained numerical values remain in good agreement with numerical data. Last, but not least, the impact of TCR on temperature distribution in rotors was analyzed for different rotational speeds. The research has confirmed a marked influence of TCR on heat transfer in blade roots due to the bottleneck effect, and the further research should be undertaken into vane geometry.

Acknowledgments

The present work is a part of the joint research program COOREFLEX-Turbo within the framework of AG Turbo. This work is supported by the German Ministry of Economy and Technology under grant number 03ET7041B. The authors gratefully acknowledge GE Power for their support and permission to publish this paper. The responsibility for the content of this publication lies with the corresponding authors.

References

[1] H. Wirth, K. Schneider, Recent facts about photovoltaics in germany, Fraunhofer ISE (2015) 92.

[2] J. Vogt, T. Schaaf, W. Mohr, K. Helbig, Flexibility improvement of the steam turbine of conventional or ccpp, Power-Gen Europe, Cologne, Germany, June (2013) 4–6.

[3] S. Flake, et al., Using stream turbine warming blankets to reduce startup time and rotor stress, Power 160 (3) (2016) 14–17.

[4] J. Spelling, M. Jöcker, A. Martin, Thermal modeling of a solar steam turbine with a focus on start-up time reduction, Journal of engineering for gas turbines and power 134 (1) (2012) 013001.

[5] M. Topel, M. Genrup, M. Jöcker, J. Spelling, B. Laumert, Operational improvements for startup time reduction in solar steam turbines, Journal of Engineering for Gas Turbines and Power 137 (4) (2015) 042604.

[6] K. Helbig, C. KÜHNE, W. Mohr, A warming arrangement for a steam turbine in a power plant, eP Patent App. EP20,120,195,309 (Jun. 4 2014).

[7] L. He, M. Oldfield, Unsteady conjugate heat transfer modeling, Journal of turbomachinery 133 (3) (2011) 031022.

[8] D. Toebben, P. Łuczyński, M. Diefenthal, M. Wirsum, S. Reitschmidt, W. F. Mohr, K. Helbig, Numerical investigation of the heat transfer and flow phenomena in an ip steam turbine in warm-keeping operation with hot air, in: ASME Turbo Expo 2017: Turbomachinery Technical Conference and Exposition, American Society of Mechanical Engineers, 2017, pp. V008T29A014–V008T29A014.

[9] M. Diefenthal, P. Łuczyński, C. Rakut, M. Wirsum, T. Heuer, Thermomechanical analysis of transient temperatures in a radial turbine wheel, Journal of Turbomachinery 139 (9) (2017) 091001.

[10] M. Diefenthal, P. Łuczyński, M. Wirsum, Speed-up methods for the modeling of transient temperatures with regard to thermal and thermomechanical fatigue, in: 12th European Turbomachinery Conference, 2017.

[11] D. Bohn, J. Ren, K. Kusterer, Conjugate heat transfer analysis for film cooling configurations with different hole geometries, ASME Paper No. GT2003-38369.

[12] D. Bohn, T. Heuer, K. Kusterer, Conjugate flow and heat transfer investigation of a turbo charger, Journal of engineering for gas turbines and power 127 (3) (2005) 663–669.

[13] K. Saunders, S. Alizadeh, L. Lewis, J. Provins, The use of cfd to generate heat transfer boundary conditions for a rotor-stator cavity in a compressor drum thermal model, in: ASME Turbo Expo 2007: Power for Land, Sea, and Air, American Society of Mechanical Engineers, 2007, pp. 1299–1310.

[14] L. V. Lewis, J. I. Provins, A non-coupled cfd-fe procedure to evaluate windage and heat transfer in rotor-stator cavities, ASME Paper No. GT2004-53246.

[15] M. Diefenthal, C. Rakut, H. Tadesse, M. Wirsum, T. Heuer, Temperature gradients in a radial turbine in steady state and transient operation, in: International gas turbine conference, Tokyo, Japan, 2015.

[16] H. D. Baehr, K. Stephan, Wärme-und stoffübertragung, Wärme-und Stoffübertragung:, ISBN 978-3-642-05500-3. Springer-Verlag Berlin Heidelberg, 2010.
[17] D. Többen, X. E. R. de Graaf, P. Łuczyński, M. Wirsum, W. Mohr, K. Helbig, Test rig for applied experimental investigations of the thermal contact resistance at the blade-rotor-connection in a steam turbine, ISROMAC.
[18] M. M. Yovanovich, Four decades of research on thermal contact, gap, and joint resistance in microelectronics, IEEE transactions on components and packaging technologies 28 (2) (2005) 182–206.
[19] H. Fenech, W. Rohsenow, Prediction of thermal conductance of metallic surfaces in contact, journal of Heat Transfer 85 (1) (1963) 15–24.
[20] B. B. Mikic, W. M. Rohsenow, Thermal contact resistance, National Aeronautics and Space Administration,.
[21] M. M. Yovanovich, H. Fenech, Thermal contact conductance of nominally flat, rough surfaces in a vacuum environment, Thermophysics and Temperature Control of Spacecraft and Entry Vehicles 18 (1966) 773–794.
[22] M. Cooper, B. Mikic, M. Yovanovich, Thermal contact conductance, International Journal of heat and mass transfer 12 (3) (1969) 279–300.
[23] C. V. Madhusudana, Thermal contact conductance.
[24] V. Ustinov, R. Kneer, F. Al-Sibai, S. Schulz, E. El-Magd, Influence of surface roughness on contact heat transfer, in: 2010 14th International Heat Transfer Conference, American Society of Mechanical Engineers, 2010, pp. 305–312.
[25] V. Ustinov, S. G. Schulz, R. Kneer, E. El-Magd, Model development for the contact pressure dependent heat transfer, MTZ worldwide 79 (9) (2011) 48–53.

Nomenclature

α Heat transfer coefficient

$\bar{s}$ Characteristic length for heat transfer

$\bar{T}$ Surface average temperature

ΔT Temperature difference

$\dot{\phi}$ Rotational speed

$\dot{Q}$ Heat rate

λ Thermal conductivity

ν Kinematic viscosity

Φ Flow coefficient

ρ Density

$\underline{T}$ Volume average temperature

$-\infty/\infty$ Time point before the start/at the end of pre-warming

A Area

a Thermal diffusivity

AP Air pockets

av Average

ax Axial

Bi Biot-number

C Contact

C_p Specific heat

CFD Computational fluid dynamics

CFL Courant-Friedrichs-Lewy

CHT Conjugate heat transfer

CI Contact interfaces

D Domain

ET Equalized Timescales

FEA Finite element analysis

FEM Finite element method

FL Fluid

Fo Fourier-number

H Housing

HTC Heat transfer coefficient

i Surface

IP Intermediate-pressure

l Characteristic length for turbine flow

n Inlet plane of a cascade

Nu Nusselt-Number

OP Operating point

p Pressure

R Rotor

r_1/r_2 Inner/Outer flow channel radius

Re Reynolds-number

RES Renewable energy sources

S Stator

SF Speed up factor

SL Solid

T Temperature

TCR Thermal contact resistance

TS Time step

u Circumferential

V Volume

v Velocity